

Research Article

Open Access

Jakub Zdarta, Karina Sałek, Agnieszka Kołodziejczak-Radzimska, Katarzyna Siwińska-Stefańska, Karolina Szwarc-Rzepka, Małgorzata Norman, Łukasz Kłapiszewski, Przemysław Bartczak, Ewa Kaczorek, Teofil Jesionowski*

Immobilization of *Amano Lipase A* onto Stöber silica surface: process characterization and kinetic studies

Abstract: The immobilization of *Amano Lipase A* from *Aspergillus niger* by adsorption onto Stöber silica matrix obtained by sol-gel method was studied. The effectiveness of the enzyme immobilization and thus the usefulness of the method was demonstrated by a number of physicochemical analysis techniques including Fourier Transform Infrared Spectroscopy (FT-IR), elemental analysis (EA), thermogravimetric analysis (TG), porous structure of the support and the products after immobilization from the enzyme solution with various concentration at different times. The analysis of the process' kinetics allowed the determination of the sorption parameters of the support and optimization of the process. The optimum initial concentration of the enzyme solution was found to be 5 mg mL⁻¹, while the optimum time of the immobilization was 120 minutes. These values of the variable parameters of the process were obtained by as ensuring the immobilization of the largest possible amount of the biocatalyst at the most economically beneficial aspects of the process.

Keywords: enzyme immobilization by adsorption, *Amano Lipase A*, silica, immobilization kinetic

DOI: 10.1515/chem-2015-0017
received March 21, 2014; accepted June 3, 2014.

*Corresponding author: Teofil Jesionowski: Institute of Chemical Technology and Engineering, Faculty of Chemical Technology, Poznan University of Technology, 60965 Poznan, Poland, E-mail: teofil.jesionowski@put.poznan.pl

Jakub Zdarta, Karina Sałek, Agnieszka Kołodziejczak-Radzimska, Katarzyna Siwińska-Stefańska, Karolina Szwarc-Rzepka, Małgorzata Norman, Łukasz Kłapiszewski, Przemysław Bartczak, Ewa Kaczorek: Institute of Chemical Technology and Engineering, Faculty of Chemical Technology, Poznan University of Technology, 60965 Poznan, Poland

1 Introduction

Lipases are widely used as natural biocatalysts mainly in the hydrolysis of triglyceride chains [1]. Among others, the cleavage of the ester bond is of great importance for biodiesel production, synthesis of pharmaceuticals and cosmetics and in many branches of the food industry [2]. Low thermal stability, narrow pH range and a fast decrease in the catalytic activity are the main factors that limit the industrial use of lipases [3,4]. Lipase immobilization has been proposed to improve its stability and activity [5,6]. Among many methods proposed for protein immobilization, the most important and useful is immobilization by adsorption [7-9].

The greatest advantage of this method is its low cost, universality and a wide range of possible supports showing good adsorption properties [10]. The supports can be either synthetic materials (mainly silicas) [11,12] or natural ones such as chitin and chitosan [13-15]. They are also characterized by high stability, well-developed surface area, and the possibility of surface functionalization with many modifying compounds [16,17]. Due to the unique properties of such materials, especially highly ordered mesoporous structures, they are widely used in the enzyme immobilization [18-20].

Among many silica supports of different structures, much interest has been paid to mesoporous silica SBA-15. The adsorption of lipase from *Candida* sp. 99-125 on this matrix, functionalized with silane was described [21]. The matrix with the immobilized biocatalyst showed over 70% of the original catalytic activity even after eight catalytic cycles, while the free enzyme lost activity after three cycles. The process of immobilization of the lipase from *Candida antarctica* on the same matrix was performed and the product kept its catalytic activity after eight catalytic cycles [22].

Interesting results have been obtained for lipases immobilized on the sol-gel silica activated by multi-walled carbon nanotubes, which permitted their use in organic solvents [23]. The activity of lipases immobilized on the modified silica was seven times higher compared to the system without the modifying agent. The lipase from *Candida rugosa* immobilized on hexagonal mesoporous silica – MSU-H [24] was used in organic media, the content of the immobilized enzyme on the samples obtained was up to 64.5 mg of the protein per 1 g of the support.

The silica support was used for immobilization by adsorption of *Burkholderia cepacia* lipase. The products showed an increased stability and prolonged catalytic activity. The amount of the immobilized enzyme proved not to be directly related to the catalytic activity, e.g. the product containing 25 mg of enzyme per 1 g of the support showed the same activity as the one containing 120 mg of the enzyme per 1 g of the matrix [25].

The aim of this paper was to present a comprehensive analysis of the immobilization of *Amano Lipase A* from *Aspergillus niger* by adsorption onto Stöber silica surface. The support was fully characterized for its physicochemical and dispersive-morphological properties and the effectiveness of the proposed immobilization method was presented. Particular attention was paid to the kinetic analysis of the process in order to establish the amount of immobilized enzyme, optimum time of the process and sorption capacity of the support. In the hitherto published literature the kinetics of immobilization has not yet been of much interest.

2 Experimental procedure

2.1 Reagents

Tetraethoxysilane (TEOS), 96% ethyl alcohol and 85% phosphoric acid were purchased from Chempur company. Phosphate buffer at pH = 7 was obtained from Amresco company. *Amano Lipase A* (ALA) from *Aspergillus niger*, 25% solution of ammonia, 4-nitrophenyl palmitate, gum arabic, Triton X-100 and Coomassie Brilliant Blue were purchased from Sigma-Aldrich (USA).

2.2 Analysis

The surface morphology and microstructure of silica was examined on the basis of the SEM image recorded from an

EVO40 scanning electron microscope (Zeiss, Germany). Before testing, the sample was coated with Au for a time of 5 seconds using a Balzers PV205P coater (Switzerland). The dispersive properties of the obtained product were characterized with a Zetasizer Nano ZS (0.6–6000 nm) made by Malvern Instruments Ltd. (UK), employing the non-invasive backscatter technology.

A thermogravimetric analyzer (TG, model Jupiter STA 449F3, made by Netzsch, Germany) was used to investigate the thermal stability of the sample. Measurements were carried out under nitrogen flow (10 mL min⁻¹) at a heating rate of 10°C min⁻¹, and a temperature range of 25 – 1000°C with an initial sample weight of approximately 5 mg.

In order to characterize the parameters of the porous structure of the obtained silica, such as: surface area, pore volume and average pore size an ASAP 2020 instrument from Micromeritics Instrument Co. (USA) was used. The surface area was determined by the multipoint BET (Brunauer–Emmett–Teller) method using data for adsorption under relative pressure (p/p_0). The BJH (Barrett–Joyner–Halenda) algorithm was applied to determine the size of pores.

The presence of the expected functional groups was examined by means of Fourier transform infrared spectroscopy (FT-IR), recorded on a Vertex 70 spectrometer (Bruker, Germany). The material was analyzed in the form of tablets, made by pressing a mixture of anhydrous KBr (ca. 0.25 g) and 1 mg of the tested substance in a special steel ring under a pressure of approximately 10 MPa. The investigation was performed at a resolution of 0.5 cm⁻¹.

UV-Vis spectroscopy (UV-1601 PC Shimadzu, Japan) was used in order to calculate the kinetic studies and protein concentrations according to Bradford method [26].

The elemental composition of the products was established using a Vario EL Cube instrument (Elementar Analysensysteme GmbH, Germany), which is capable of recording the carbon, hydrogen and nitrogen content in samples following their high-temperature combustion.

The zeta potential was measured with a Zetasizer Nano ZS (Malvern Instruments Ltd., UK) equipped with an autotitrator. The measurements were performed in a 0.001M solution of NaCl. This instrument employs a combination of electrophoresis and laser measurement of particle mobility based on the Doppler phenomenon. The speed of particles moving in a liquid under electric field, known as the electrophoretic mobility, was measured. Then, the value of the zeta potential was calculated from the Smoluchowski equation.

2.3. Preparation of silica

Silica was synthesized by a modified Stöber method [27]. The process involves the reaction of tetraethoxysilane (TEOS) in the medium of a 96% ethyl alcohol in the presence of a 25% ammonium hydroxide solution as a catalyst. The reaction was conducted at 40°C for 30 minutes. A mixture of ethanol and ammonium hydroxide at the ratio 10:1 was stirred in the reactor, into which TEOS was introduced in doses. After completion of the process the product was filtered off under the reduced pressure and then washed out a few times with ethyl alcohol and finally dried out at 105°C for 24 hours.

2.4 Immobilization of *Amano Lipase A* onto silica surface

A portion of the support, the same amount for all samples, was placed in the reactor and then 15 mL of a solution of *Amano Lipase A* of a given concentration (1; 3; 5; 7 mg mL⁻¹) in a phosphate buffer of pH = 7 was added. The mixture was mounted on a shaker and the process of adsorption was taking place for a certain time, varied from 1 minute to 96 hours. After the process, the mixtures were filtered off under reduced pressure. The precipitate being the silica support with the immobilized enzyme was dried at ambient temperature for 24 hours and then subjected to further analyses, while the filtrate was subjected to a spectrophotometric analysis.

2.5 Evaluation of the hydrolytic activity of *Amano Lipase A* after the immobilization onto Stöber silica support

The hydrolytic activity of the immobilized enzymes was estimated according to Matte *et al.* [28]. Briefly, the spectrophotometric measurements were based on the ability of the enzymes to transform the p-NPP (para-nitrophenyl palmitate) into pNP (para-nitrophenol). The release of the product was observed at 410 nm. The enzymatic activity was measured in quartz cuvettes containing 3 to 5 mg of silica with the immobilized lipases and 2.7 mL of working solution (10 mM phosphate buffer, 10 mM pNPP solution in 2-propanol, 0.44% mass fraction of Triton X-100, Arabic gum – 0.11% mass fraction). All reactions (performed in triplicate) were carried out with stirring at 1000 rpm, at 30°C and for 2 minutes. One unit of the enzyme activity was defined as the release of 1 mmol of pNP per one minute under the measurement conditions.

3 Results and discussion

3.1 Physicochemical analysis of silica support

The obtained silica was subjected to a thorough examination of its physicochemical and dispersive-morphological properties. As follows from the SEM image, (Fig. 1), the silica is made of uniform and spherical shape particles. The microscopic observations are confirmed by the analysis of volume contributions of different size particles on a Zetasizer Nano ZS. The range of particle diameters determined by non-invasive back-scatter (NIBS) optics is 220 – 531 nm, and the particles of diameter 295 nm bring the maximum volume contribution of 21.4%. Thus, the silica support obtained by the sol-gel method is homogeneous.

3.2 Silica characterization after the immobilization of the *Amano Lipase A*

3.2.1 FT-IR analysis

The silica and the enzyme were subjected to FT-IR analysis. Their spectra are presented in Fig. 2.

The spectrum of the support reveals five characteristic signals of silica. One of them seen at 3748 cm⁻¹, comes from the isolated silanol group vibrations \equiv Si-OH. The second signal at 1120 cm⁻¹ is assigned to the stretching vibrations of \equiv Si-O- group [29]. The other three signals appear between 1000 cm⁻¹ and 469 cm⁻¹, and are assigned to the asymmetric and symmetric bending vibrations and stretching vibrations of \equiv Si-O-Si= group [30]. There is also a broad band in the range 3500 and 3200 cm⁻¹, assigned to the stretching vibrations of hydroxyl groups and a signal at 1620 cm⁻¹ assigned to water physically adsorbed on the SiO₂ surface.

The FT-IR spectrum of *Amano Lipase A* from *Aspergillus niger* shows many signals characteristic for different functional groups of the enzyme. They include a typical band at 2930 cm⁻¹ assigned to the stretching C-H vibrations of -CH₂ and -CH₃ groups, a broad and intense band between 3600 and 3200 cm⁻¹ assigned to the stretching vibrations of -OH group, and a band of the -N-H stretching vibrations, masked by the former one. The characteristic signals coming from the stretching vibrations of carbonyl groups around 1700 cm⁻¹ and stretching vibrations of \equiv C-O- appear in the spectrum at 1180 cm⁻¹. The signal assigned to the deformation vibrations of -NH group is seen at 1550 cm⁻¹ [31], while the signal of the -OH deformation vibrations appears at 1400 cm⁻¹. Below

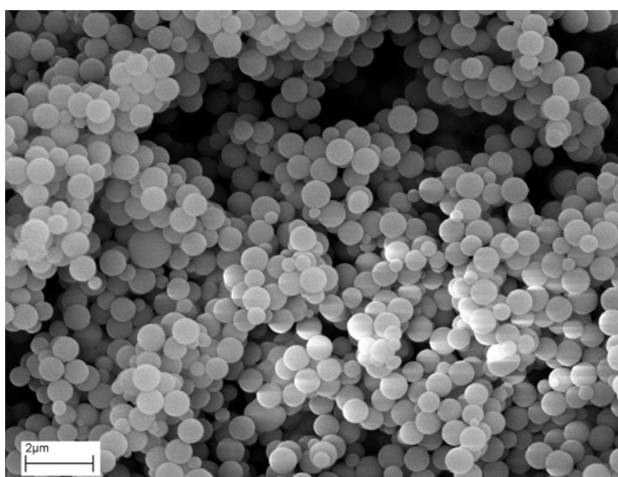


Figure 1: SEM image of obtained Stöber silica support.

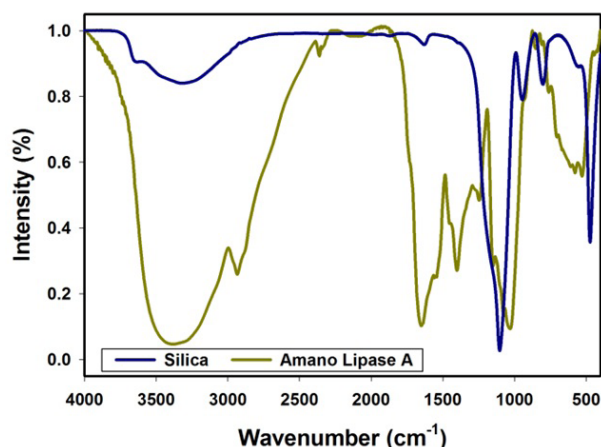


Figure 2: FT-IR spectra of silica and *Amano Lipase A*.

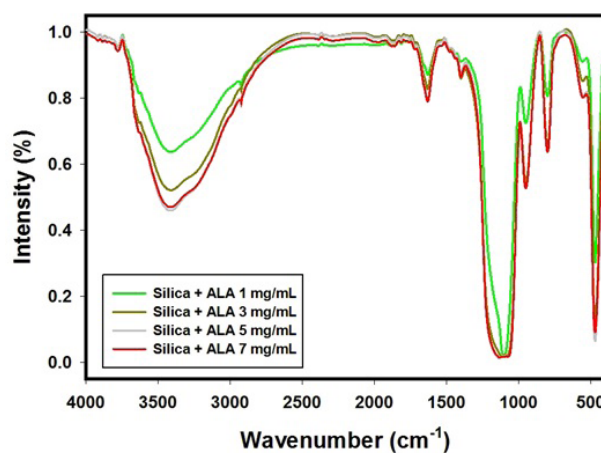


Figure 3: FT-IR spectra of silica after *Amano Lipase A* immobilization.

1000 cm⁻¹ there are a few signals assigned to the carbon-carbon bonds. Analysis of the FT-IR spectrum of the enzyme confirmed the presence of a number of functional groups in the enzyme structure, which can be employed for binding the enzyme to the appropriately modified support.

The enzyme immobilization by adsorption onto the silica support was performed for the enzyme solutions in different concentrations and for different time stages of the process. After completion of immobilization the samples were subjected to FT-IR spectroscopic analysis. The results are presented in Fig. 3.

The FT-IR spectra of silica with immobilized enzyme show the bands of silica at 3748 cm⁻¹ and 1120 cm⁻¹, and between 1000 cm⁻¹ and 469 cm⁻¹. Apart from the above mentioned bands, there are some of those present in the spectrum of the pure enzyme, such as the two signals at 1450 cm⁻¹ and 1490 cm⁻¹ assigned to the scissor vibrations of \equiv C-H groups and a signal at 2920 cm⁻¹ generated by the C-H symmetric stretching vibrations of $-CH_2$ and $-CH_3$ groups. Also, the most important and characteristic for the pure enzymes are the amide I and amide II bands seen at 1645 cm⁻¹ and 1542 cm⁻¹ respectively [32,33]. After the immobilization, those bands were not only noticed to have their intensities decreased, but also their wave numbers (cm⁻¹) slightly shifted to 1637 and 1536 cm⁻¹, respectively.

These changes indicate that the adsorption on the silica matrix successfully took place [34] and one can draw some conclusions on the secondary structure of the peptide after the immobilization [35,36]. The presence of amide I and amide II bands may also be proof that the immobilized enzyme could have preserved its activity [36].

The above FT-IR spectra were recorded for the samples obtained after 2 hours of immobilization as it was found to be the optimum time for the process. The analysis of the spectra show that the amount of immobilized enzyme depends on the enzyme concentration in the initial solution. The intensities of the bands assigned to the immobilized enzyme increase for the initial solutions of the enzyme concentrations 1, 3 and 5 mg mL⁻¹, while such an increase is not observed for the sample obtained from the initial solution of 7 mg mL⁻¹, as the bands intensities are the same as in the spectrum of the sample obtained from the initial solution concentration of 5 mg mL⁻¹.

3.2.2 TG analysis

The samples of silica, lipase and immobilized enzymes were subjected to thermogravimetric analysis to determine their thermal stability, which is important

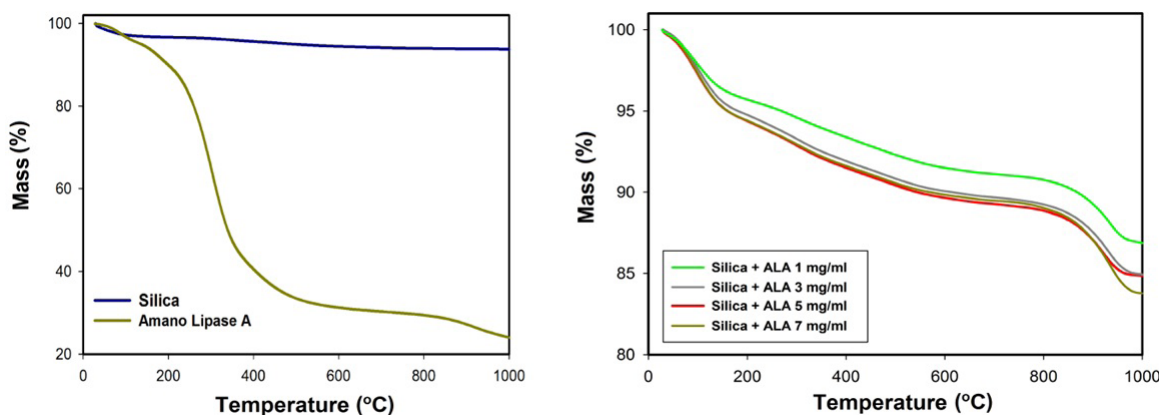


Figure 4: TG curves of the silica support and *Amano Lipase A* after immobilization.

when considering the application of these systems as biocatalysts. The results are illustrated in Fig. 4.

The TG curve recorded for SiO_2 indicates a small mass loss of about 5%, confirming the high thermal stability of the silica [25]. The TG data of *Amano Lipase A* data suggest that the weight loss is about 65%. The obtained products are characterized by relatively high thermal stability. The TG curves of immobilized samples show two stages. The first stage is between 20 and 200°C, and the second from around 800°C. The first stage corresponds to the loss of water adsorbed on the surface of the materials, while the second stage corresponds to the thermal decomposition of lipase that was adsorbed on the silica surface [37,38].

The TG curves of products after immobilization show that for the higher concentration of the adsorbed enzyme the lower thermal stability of the system is detected. Assuredly, this is related to the amount of adsorbed enzyme on the silica surface. The data obtained from thermal analysis additionally confirms the effectiveness of the performed immobilization process.

3.2.3 Elemental analysis

To verify the effectiveness of immobilization, the samples were subjected to elemental analysis bringing the information on the percentage content of such elements as nitrogen, carbon and hydrogen. The results of elemental analyses performed for the samples obtained for the initial enzyme solution of the concentration 5 mg mL^{-1} and for different times of immobilization are presented in Table 1.

The silica obtained by the sol-gel method and used as a support was found to contain 1.30% of hydrogen with no carbon and no nitrogen. The data obtained for the

sample after enzyme immobilization prove an increasing content of carbon and hydrogen and the appearance of nitrogen in the elemental composition, which confirms the effectiveness of lipase immobilization. The content of the above mentioned elements increase along with the time of immobilization process for the times 1, 60 and 120 minutes. For the other two immobilization times, the contents of the elements remain at similar levels and do not increase.

3.2.4 Zeta potential

The electrokinetic properties of the silica support and the product of enzyme immobilization were characterized on the basis of zeta potential measurements, performed in the pH range 2 to 10.

Fig. 5 presents the pH dependence of zeta potential measured for the silica support obtained by the sol-gel method and for the pure enzyme. The zeta potential of the silica support decreases with increasing pH, reaching -45 mV for pH = 10. Therefore, the SiO_2 dispersion is stable in the neutral and alkaline media. The potential generating ions in the silica are H^+ and OH^- . The isoelectric point is close to 4.5. According to Arino *et al.*, the isoelectric point of native lipase from *Aspergillus niger* is 4.4 [39]. Electrokinetic potential of ALA is negative in the entire pH range studied and the maximum absolute value of the potential does not exceed 15 mV, which indicates the instability of the biocatalyst in the pH range studied. It should be added that for pH above 7 no zeta potential measurement could be made, which suggests its high instability and biocatalyst decomposition already in weakly alkaline media.

Fig. 6 shows the pH dependence of zeta potential measured for the sample of silica with immobilized enzyme, obtained by adsorption from the 5 mg mL^{-1}

solution, for different times of the adsorption process [40]. These electrokinetic curves were compared with those measured for the silica and the native enzyme. The isoelectric points of the silica with immobilized enzyme are similar, irrespective of the time of immobilization [41]. The isoelectric point and zeta potential reach similar values when compared to those obtained for the silica support [42,43]. The shapes of the electrokinetic curves obtained for the silica with immobilized enzyme are similar to that recorded for the silica support [44]. The zeta potential of silica with immobilized enzyme reaches the absolute values higher than 30 mV for pH above 6, which shows a high electrokinetic stability of the samples in this pH range.

3.2.5 Porous structure analysis

To characterise the adsorption capacity of the silica and silica with immobilized enzyme, the porous structure of these samples was determined. The results given in Table 2 refer to the samples of silica with immobilized enzyme adsorbed from the 5 mg mL^{-1} solution for different times of adsorption.

The results confirm the effectiveness of the proposed method of enzyme immobilization, evidenced by a decrease in surface area, pore size and pore volume as a consequence of enzyme immobilization. The data confirm that the optimum time of adsorption is 120 minutes. After this time no significant changes are observed in the above mentioned parameters, which mean that no more enzyme could be adsorbed. The decrease in the values of these parameters can also suggest both physisorption or chemisorption interactions between the enzyme and reactive groups of silica.

3.2.6 Amount of enzyme adsorbed

The amount of enzyme adsorbed was determined according to the Bradford method [26]. After a series of spectrophotometric measurements, the concentration of the enzyme left in the solution after immobilization was read off the plot of absorbance versus enzyme concentration. On the basis of the known amount of sorbent, volume and concentration of the initial enzyme solution it was possible to calculate the amount of enzyme immobilized on the silica support. The results in mg of enzyme per 1 g of the support are given in Table 3.

The amounts of immobilized enzyme in the obtained products, using the enzyme solutions of different

Table 1: Results of elemental analysis of silica after *Amano Lipase A* immobilization.

Sample name	Elemental content (%)		
	N	C	H
Stöber silica	-	-	1.30
Silica + ALA (1 min)	0.09	0.62	1.49
Silica + ALA (60 min)	0.10	0.69	1.53
Silica + ALA (120 min)	0.14	0.89	1.78
Silica + ALA (24 h)	0.15	0.90	1.79
Silica + ALA (96 h)	0.15	0.91	1.79

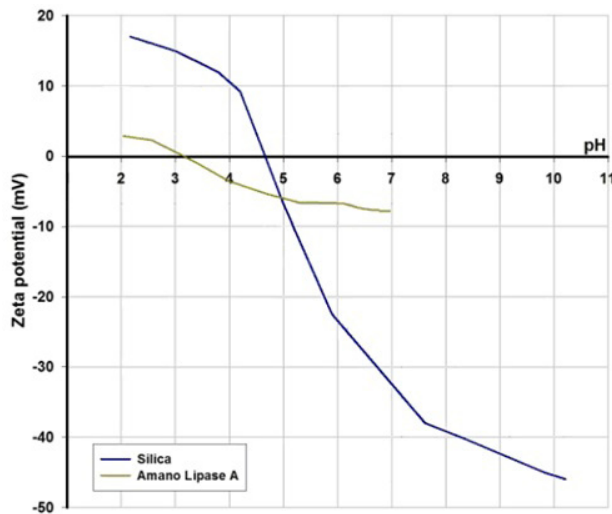


Figure 5: Zeta potential of Stöber silica and *Amano Lipase A*.

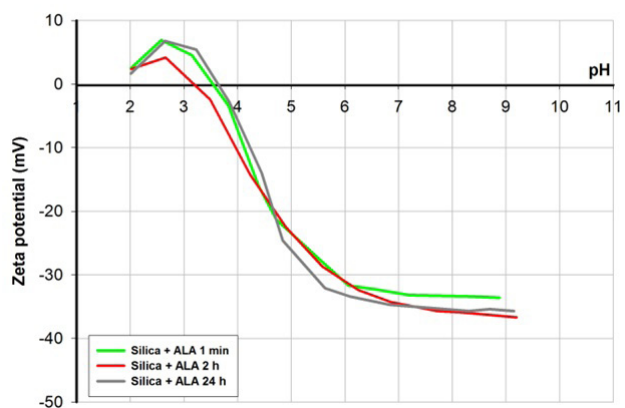


Figure 6: Zeta potential vs. pH of the silica with immobilized *Amano Lipase A*.

concentrations and different times of adsorption, are given in Table 3. The data indicate that the enzyme adsorption on the silica surface is the most intense in the time from

Table 2: Parameters of porous structure of both silica and silica after enzyme immobilization.

Sample name	BET surface area ($\text{m}^2 \text{g}^{-1}$)	Total volume of pores ($\text{cm}^3 \text{g}^{-1}$)	Mean size of pores (nm)
Stöber silica	9.8	0.007	2.8
Silica + ALA (1 min)	5.8	0.004	2.5
Silica + ALA (60 min)	4.9	0.004	2.0
Silica + ALA (120 min)	4.0	0.003	1.9
Silica + ALA (24 h)	3.9	0.003	1.9
Silica + ALA (96 h)	3.9	0.003	1.8

1 to 60 minutes of the process and after 120 minutes no significant increase in the amount of the enzyme adsorbed is noted. Interestingly, the higher the initial enzyme concentration in solution is, the faster the increase in the amount of immobilized enzyme in the same time of the process is noted. Also, the amount of the enzyme immobilized on the silica increases with increasing initial enzyme concentration in the solution. For the process of immobilization from the solution of the enzyme concentration of 1 mg mL^{-1} after 120 minutes, there is 18 mg of the enzyme per 1 g of silica, which is much greater than that reported by Galarneau *et al.* [45]. If the enzyme concentration in the initial solution is 3 mg mL^{-1} , after the same time of 120 minutes, we get 63 mg of the enzyme per 1 g of silica. After 120 minutes of the process performed from the solution of the enzyme concentration 5 mg mL^{-1} , there is 122 mg of the enzyme per 1 g of silica, and if the process is performed from the solution of enzyme concentration 7 mg mL^{-1} there is 157 mg of the enzyme per 1 mg of sol-gel silica. As follows, the amount of enzyme immobilized on silica increases with an increasing initial concentration of the enzyme in solution, but for the solutions of the highest concentrations used, the difference is not so visible.

3.2.7 Hydrolytic activity

The hydrolytic activity of free and immobilized lipases was spectrophotometrically assayed as described in part 2.5. The initial concentrations of the lipase solutions used in this experiment were: 1 mg mL^{-1} ; 3 mg mL^{-1} ; 5 mg mL^{-1} ; and 7 mg mL^{-1} . The times of the immobilization process for this experiment were: 2, 24 and 96 hours.

It turns out that the best incubation time of the samples consisting of silica and the appropriate amounts of the enzyme is 24 hours (Table 4). That is shown by samples 1 – 5, where the highest activity of lipases was observed after 24-hours of the sample incubation. However, when the highest initial enzyme concentration

Table 3: Amounts of immobilized enzyme.

Enzyme concentration	1 mg mL^{-1}	3 mg mL^{-1}	5 mg mL^{-1}	7 mg mL^{-1}
Sample name	Amount of immobilized enzyme (mg/g)			
Silica + ALA (1 min)	6	15	10	25
Silica + ALA (10 min)	15	47	61	92
Silica + ALA (60 min)	17	62	118	155
Silica + ALA (120 min)	18	63	122	157
Silica + ALA (24 h)	18	63	122	158
Silica + ALA (96 h)	19	64	123	158

was applied, the loss of the enzyme activity was incredibly significant (from 7.218 mU to 1.115 mU – just 20 hours later). This result may indicate that the adsorption of such a high initial amount of the enzyme (7 mg mL^{-1}) could be very unstable and temporary and the longer the samples were under shaking, the higher detachment of the enzyme from the silica could have taken place.

What is more, as indicated in many reports, the hydrolytic activity of the lipases does not only depend on the temperature, but also on the pH of the solution during the incubation process and/or the activity measurements. This work however, presents the first measurements of the lipase activity for the immobilization by adsorption obtained by our team and will be thoroughly studied in the next steps of our work.

3.3 Kinetic studies

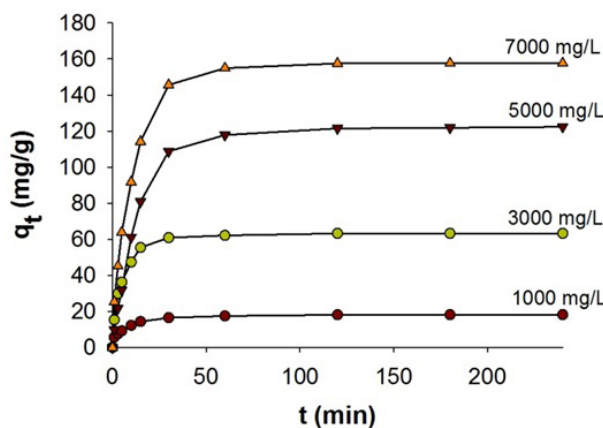
The amount of enzyme adsorbed per a time unit (q_t) is calculated from the equation:

$$q_t = \frac{(C_0 - C_t) \cdot V}{m} \quad (1)$$

where C_0 and C_t are the concentrations of the enzyme (mg L^{-1}) in the solution before and after adsorption

Table 4: Hydrolytic activity.

Sample name	Immobilization time (h)	Hydrolytic activity (mU)	Δq (%)
Silica + ALA 1	2	1.657	0.607
	24	4.018	0.667
	96	3.500	0.448
Silica + ALA 3	2	1.444	0.114
	24	3.351	0.839
	96	3.110	1.051
Silica + ALA 5	2	0.722	0.059
	24	1.455	0.082
	96	1.295	0.122
Silica + ALA 7	2	7.218	1.529
	24	1.115	0.271
	96	0.390	0.136

**Figure 7:** Effect of contact time on the amount of enzyme adsorbed on the Stöber silica (enzyme concentration 1000 – 7000 mg L⁻¹, support use 0.5 g).

respectively, V is the volume of the solution (L) and m is the mass of the Stöber silica support (g). The value of q_e is needed to establish the kinetic model of the reaction, e.g. the pseudo-first-order [46] or pseudo-second-order equations [47].

To get the adsorption isotherms it was necessary to find the equilibrium concentration (q_e) of the enzyme adsorbed on the silica matrix from the following equation:

$$q_e = \frac{(C_0 - C_e) \cdot V}{m} \quad (2)$$

where q_e is the amount of enzyme adsorbed at equilibrium (mg g⁻¹), C_0 is the initial concentration of enzyme (mg L⁻¹), C_e is the equilibrium enzyme concentration (mg L⁻¹), V is

the volume of solution (L) and m is the mass of the support (g).

The standard deviation Δq (%) for the kinetic model of pseudo-second order was calculated as well, and it was in direct correlation with experimental data. Δq (%) was calculated as:

$$\Delta q(\%) = 100 \sqrt{\frac{\sum [(q_{\text{exp}} - q_{\text{cal}})/q_{\text{exp}}]^2}{N-1}} \quad (3)$$

where N is the number of data points.

The value of standard deviation ranged from 3.5 to 7.6.

3.3.1 Adsorption kinetic

The prediction of the batch sorption kinetics is needed for the process design, in particular if the immobilization is performed by an adsorption. The character of the adsorption considerably depends on the physicochemical properties of the matrix (here the sol-gel silica) and on the process parameters – especially on the time of the process. The most often used models for adsorption kinetics are the pseudo-first-order model and pseudo-second-order model. In the present study the pseudo-first-order and pseudo-second-order model were used. The model was chosen on the basis of the best fit to the experimental data, characterized by the determination coefficient (r^2).

Fig. 7 shows a plot of the amount of the enzyme adsorbed (mg g⁻¹) versus contact time for different initial enzyme concentrations.

The data above show that for each enzyme concentration in the initial solution used in the study (1000 – 7000 mg L⁻¹) the adsorption equilibrium was achieved after 120 minutes. The kinetic parameters of adsorption were determined based on the equations of the pseudo-first order kinetic model by Lagergren and pseudo-second order kinetic model by Ho and McKay.

3.3.1.1 Pseudo-first order kinetic

The Lagergren pseudo-first-order kinetic model has been widely used to predict the sorption kinetics. The enzyme adsorption kinetics following the pseudo-first-order model is given by Eq. 4:

$$\frac{dq_t}{dt} = k_1 (q_e - q_t) \quad (4)$$

where q_e and q_t (mg g⁻¹) are the amounts of the enzyme adsorbed at equilibrium and at time t (min), respectively

Table 5: Pseudo-first-order and pseudo-second-order kinetic parameters and the coefficient of determination for adsorption of enzyme onto silica.

Type of kinetic	Parameters		Concentration of enzyme (mg L ⁻¹)			
	symbols	units	1000	3000	5000	7000
Pseudo-first-order	$q_{e,exp}$	mg g ⁻¹	18.18	63.24	122.31	157.62
	$q_{e,cal}$	mg g ⁻¹	9.37	30.40	88.30	110.72
	k_1	1 min ⁻¹	0.0404	0.0588	0.0419	0.0571
Pseudo-second-order	r^2	—	0.971	0.970	0.956	0.987
	$q_{e,cal}$	mg g ⁻¹	18.53	64.21	129.20	162.74
	k_2	1 min ⁻¹	0.0134	0.0055	0.0007	0.0010
	r^2	—	0.999	0.999	0.998	0.999
	h	mg g ⁻¹ min ⁻¹	4.602	22.473	12.206	27.366
	Δq	%	3.5	3.9	7.6	6.6

and k_1 (min⁻¹) is the rate constant for the pseudo-first-order rate equation.

Eq. 4 at the boundary conditions ($qt = 0$ at $t = 0$ and $qt = qt$ at $t = t$) can be rearranged for the linearized data plotting Eq. 5:

$$\log(q_e - q_t) = \log(q_e) - \frac{k_1}{2.303}t \quad (5)$$

The equilibrium adsorption capacity (q_e) and adsorption rate constant (k_1) (Table 5) can be found from the relation $\log(q_e - q_t)$ versus t . Fig. 8 shows the plot between $\log(q_e - q_t)$ versus t .

The determination coefficient (r^2) obtained using the Lagergren pseudo-first-order kinetic model at all the initial enzyme concentrations investigated (1; 3; 5; 7 mg mL⁻¹) varied from 0.956 to 0.987 (Table 5). However, the adsorption capacity ($q_{e,cal}$) values calculated from the pseudo-first-order kinetic, were much different from the experimental capacities ($q_{e,exp}$). Much better fit was achieved assuming the pseudo-second-order kinetic model.

3.3.1.2 Pseudo-second order kinetic

The enzyme adsorption kinetics following the Ho and McKay pseudo-second-order model is given by Eq. 6:

$$\frac{dq_t}{dt} = k_2(q_e - q_t)^2 \quad (6)$$

where k_2 (g mg⁻¹ min⁻¹) is the rate constant for the pseudo-second-order rate equation and q_e and q_t are the amounts (mg g⁻¹) of the enzyme adsorbed at equilibrium and at time

t (min). Taking into account the boundary conditions ($qt = 0$ at $t = 0$ and $qt = qt$ at $t = t$) we get the integrated form of Eq. 6 as shown in Eq. 7:

$$\frac{t}{q_t} = \frac{1}{k_2 q_e^2} + \frac{1}{q_e} t \quad (7)$$

The initial adsorption rate, h (mg mg⁻¹ min⁻¹) is defined as follows:

$$h = k_2 q_e^2 \quad (8)$$

The equilibrium adsorption capacity (q_e) and adsorption rate constant (k_2) (Table 5) were found from the relation t/qt versus t . Fig. 8 shows the plot between t/qt versus t .

The fitting parameters for both the pseudo-first-order and the pseudo-second-order equations are shown in Table 5. Considering the Ho and McKay pseudo-second-order model the correlation coefficient (r^2) took values from the range 0.998 – 0.999. The adsorption capacity ($q_{e,cal}$) predicted by the pseudo-second-order model was in a very good correlation with the values of experimental capacities ($q_{e,exp}$). The kinetic parameters obtained indicate that the pseudo-second-order model represents the experimental behaviour accurately. For all initial enzyme concentrations in solutions considered in this study, the correlation coefficient (r^2) obtained for the fit with the pseudo-second-order model are higher than those obtained from the fit with the pseudo-first-order model. Assuming the pseudo-second-order model, a decrease in the rate constant of adsorption (k_2) and in the initial sorption rate (h) was observed with increasing initial concentration of the enzyme in solution. The values

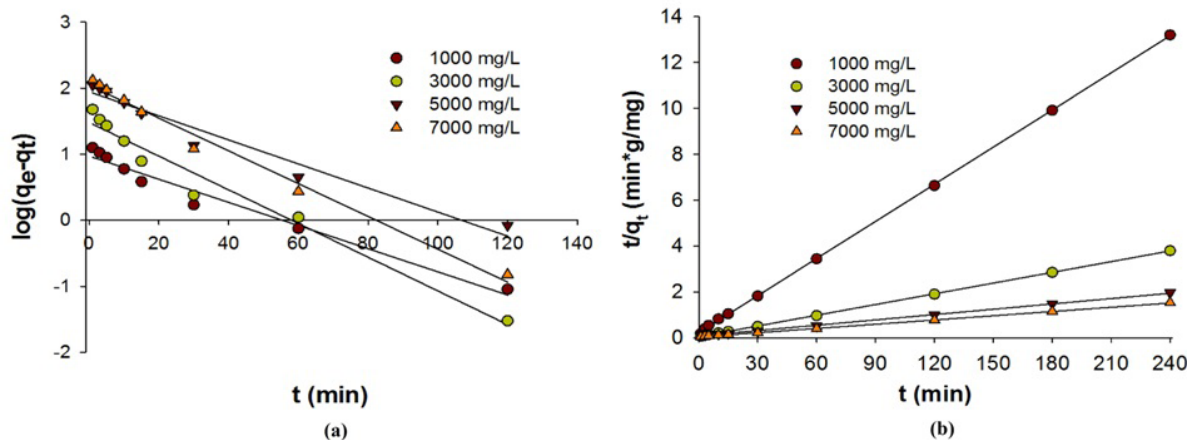


Figure 8: The fit to the adsorption of *Amano Lipase A* onto Stöber silica support using (a) pseudo-first-order and (b) pseudo-second-order model.

of k_2 and h for the initial concentration of the enzyme of 5000 mg L⁻¹ deviate from this dependence.

4 Conclusions

The immobilization of the *Amano Lipase A* from *Aspergillus niger* was studied on the silica support obtained by the sol-gel method and built of uniform particles of spherical shape. The process of ALA immobilization was performed for different times and different concentrations of the enzyme in solutions. The effectiveness of the proposed method of immobilization was verified on the basis of FT-IR spectra, thermogravimetric curves and elemental composition determination. The amount of enzyme immobilised on the silica support was found to depend on the time of the process and on the initial concentration of the enzyme in solution. The greatest increase in the amount of adsorbed enzyme is observed for the time of the process from 1 to 60 minutes. After two hours of the process no significant increase in the amount of the adsorbed enzyme is observed, thus this time was assumed as the optimum for the process.

The kinetics of *Amano Lipase A* immobilization on the silica support was found to be best described by the pseudo-second-order model, which was confirmed by the values of the correlation coefficient (r^2) of 0.998 – 0.999.

Acknowledgements: This work was supported by Poznan University of Technology research grant no. 03/32/DSMK/0462/2014.

References

- [1] Reetz M.T., *Curr. Opin. Chem. Biol.*, 2002, 6, 145
- [2] Hasan F., Shah A.A., Hameed A., *Enzyme Microb. Technol.*, 2006, 39, 235
- [3] Zhang S., Shang W., Yang X., Zhang S., Zhang X., Chen J., *Bull. Korean Chem. Soc.*, 2013, 34, 2741
- [4] Ariga K., Ji Q., Mori T., Naito M., Yamauchi Y., Abe H., Hill J.P., *Chem. Soc. Rev.*, 2013, 42, 6322
- [5] Sheldon R.A., *Adv. Synth. Catal.*, 2007, 349, 1289
- [6] Adlercreutz P., *Chem. Soc. Rev.*, 2013, 42, 6406
- [7] Rodrigues R.C., Ortiz C., Berenguer-Murcia A., Torres R., Fernandez-Lafuente R., *Chem. Soc. Rev.*, 2013, 42, 6290
- [8] Mateo C., Palomo J.M., Fernandez-Lafuente G., Guisan J.M., Fernandez-Lafuente R., *Enzyme Microb. Technol.*, 2007, 40, 1451
- [9] Fernandez-Lafuente R., *Enzyme Microb. Technol.*, 2009, 45, 405
- [10] Sheldon R.A., van Pelt S., *Chem. Soc. Rev.*, 2013, 42, 6223
- [11] Magner E., *Chem. Soc. Rev.*, 2013, 42, 6213
- [12] Hartmann M., Kostrov X., *Chem. Soc. Rev.*, 2013, 42, 6277
- [13] Krajewska B., *Enzyme Microb. Technol.*, 2004, 35, 126
- [14] Krajewska B., *Sep. Purif. Tech.*, 2005, 41, 305
- [15] Ehrlich H., Krajewska B., Hanke T., Born R., Heinemann S., Knieb C., Worch H., *J. Membr. Sci.*, 2006, 273, 124
- [16] Cipolatti E.P., Silva M.J.A., Kleina M., Feddern V., Feltes M.M.C., Oliveira J.V., et al., *J. Mol. Catal. B Enzym.*, 2014, 99, 56
- [17] Krajewska B., *J. Mol. Cat. B Enzym.*, 2009, 59, 9
- [18] Zhou Z., Hartmann M., *Chem. Soc. Rev.*, 2013, 42, 3894
- [19] Ariga K., Vinu A., Yamauchi Y., Ji Q., Hill J.P., *Bull. Chem. Soc. Jpn.*, 2012, 85, 1
- [20] Petkovich N.D., Stein A., *Chem. Soc. Rev.*, 2013, 42, 3721
- [21] Li Y., Wang W., Han P., *Korean J. Chem. Eng.*, 2014, 31, 98
- [22] Arumugam A., Ponnusami V., *J. Sol-Gel Sci. Technol.*, 2013, 67, 244
- [23] Lee S.H., Doan T.T.N., Won K., Ha S.H., Koo Y.M., *J. Mol. Catal. B: Enzym.*, 2010, 62, 169
- [24] Yu W., Fang M., Tong D., Shao P., Xu T., Zhou C., *Biochem. Eng. J.*, 2013, 70, 97

[25] Silva A.L.P., Nascimento R.G., Arakaki L.N.H., Arakaki T., *J. Non-Cryst. Solids*, 2013, 376, 139

[26] Bradford M.M., *Anal. Biochem.*, 1976, 72, 248

[27] Kłapiszewski Ł., Królik M., Jasionowski T., *Cent. Eur. J. Chem.*, 2014, 12, 173

[28] Matte C.R., Bussamara R., Dupont J., Rodrigues R.C., Hertz P.F., Ayub M.A.Z., *Appl. Biochem. Biotechnol.*, 2014, 172, 2507

[29] Jasionowski T., Przybylska A., Kurc B., Ciesielczyk F., *Dyes Pigments*, 2011, 89, 127

[30] Szwarc-Rzepka K., Marciniec B., Jasionowski T., *Adsorption*, 2013, 19, 483

[31] Svendsen A., *Biochim. Biophys. Acta*, 2000, 1543, 223

[32] Wong P.T.T., Wong R.K., Caputo T.A., Godwin T.A., Rigas B., *Proc. Nati. Acad. Sci. USA*, 1991, 88, 10988

[33] Dousseau F., Pezolet M., *Biochemistry*, 1990, 29, 8771

[34] Delfino I., Portaccio M., Della Ventura B., Mita D.G., Lepore M., *Mater. Sci. Eng. C*, 2013, 33, 304

[35] Naidja A., Liu C., Huang P.M., *J. Colloid Interface Sci.*, 2002, 251, 46

[36] Portaccio M., Della Ventura B., Mita D.G., Manolova N., Stoilova O., Rashkov I., Lepore M., *J. Sol-Gel Sci. Technol.*, 2011, 57, 204

[37] Hou C., Zhu H., Wu D., Li Y., Hou K., Jiang Y., Li Y., *Proc. Biochem.*, 2013, 40, 244

[38] Motevalizadeh S.F., Khoobi M., Shabanian M., Asadgol Z., Faramarzi M.A., Shafiee A., *Mater. Chem. Phys.*, 2013, 143, 76

[39] Marini A., Imelio N., Pico G., Romanini D., Farrugia B., *J. Chromatogr. B*, 2011, 879, 2135

[40] Rezwan K., Meier L.P., Gauckler L.J., *Biomaterials*, 2005, 26, 4351

[41] Mohanraj V.J., Barnes T.J., Prestidge C.A., *Int. J. Pharm.*, 2010, 392, 285

[42] Feng X., Patterson D.A., Balaban M., Emanuelsson E., *Colloids Surf. B*, 2013, 102, 526

[43] Ding H., Shao L., Liu R., Xiao Q., Chen J., *J. Colloid Interface Sci.*, 2005, 290, 102

[44] Wiącek A.E., *Powder Technol.*, 2011, 213, 141

[45] Galarneau A., Mureseanu M., Atger S., Renard G., Fajula F., *New J. Chem.*, 2006, 30, 562

[46] Lagergren S., *Kungl. Svenska Vetensk. Handl.*, 1898, 24, 1

[47] Ho Y.S., McKay G., *Proc. Biochem.*, 1999, 34, 451